Nonthermal Electrons and Small-Scale Plasma Perturbations during Density Limit Disruptions in the T-10 Tokamak

P.V.Savrukhin, A.V.Sushkov, S.V.Tsaun, V.V.Volkov

Russian Research Center "Kurchatov Institute", 123182, Moscow, Russia
psavruk@nfi.kiae.ru

ABSTRACT. Repetitive bursts of the non-thermal x-ray radiation (E~25-100 keV) are observed during density limit disruptions in the T-10 tokamak (R=1.5m, a=0.3m) using tangentially viewing CdTe detectors. Analysis indicated that the phenomena can be connected with forward bremsstrahlung emission of the suprathermal electrons from the plasma area around the m=2,n=1 magnetic island and non-uniform interaction of the beams with the limiters. It is arguing that nonthermal x-ray oscillations in plasma with high density can be connected with undulated movement of the electron beams trough magnetic fields with ripples during rotation of the m=2,n=1 mode.

1. Introduction

Small-scale plasma perturbations accompanying MHD modes represent one of the specific feature of the disruption instability observed in plasma with high density [1] and high magnetohydrodynamic pressure (β) [2]. The small-scale perturbations are typically identified as high frequency oscillations of the x-ray intensity and electron cyclotron emission superimposed to a large-scale helical perturbations characterised by low *m,n* wave numbers ($n=1$ - 2 , $m=1$ - 5). In contrast to the large scale MHD modes the small-scale perturbations are typically characterised by extremely narrow toroidal wavelength (e.g. $n \sim 10$ at high β [2]) and are observed most clearly at the low field side of a tokamak plasma. The small-scale oscillations are generally associated with ballooning modes destabilised in plasma area with non-favourable curvature of the magnetic field [2] or with secondary tearing modes destabilised due to the coupling of a large-scale MHD perturbations [3].

Disruptions at high density [4,5] (as well as disruptions at high β [2]) are often accompanied by bursts of the nonthermal x-ray and EC emission ($E_\gamma \sim 100\ keV$). Resent experiments in the T-10 tokamak have demonstrated that the nonthermal bursts can be connected with forward bremsstrahlung emission of the suprathermal electrons ($E_\gamma \sim 25$ - $100\ keV$) from plasma area around the $q=1$ and $q=2$ magnetic surfaces [6]. It was speculated that localised beams of the supra-thermal electrons can be induced during magnetic reconnection around the *X* points of the $m=1,\ n=1$, and $m=2,n=1$ magnetic islands. Experiments in T-10 have also indicated that the small-scale x-ray oscillations at the density limit disruptions can be connected with instabilities possibly induced by the fast electrons in a magnetised plasma. It is arguing that the oscillations can be generated due to modulation of the electron beams moving though the equilibrium magnetic field with ripples during rotation of the m=2,n=1 mode [7].

Present paper represents phenomenology of the small-scale plasma oscillations accompanying large-scale MHD modes during density limit disruptions in the T-10 tokamak (major and minor radii, $R_0 = 1.5\ m$, $a_L = 0.25$ - $0.35\ m$, accordingly, toroidal magnetic field, $B_t = 2.0$ - $2.42\ T$, plasma current, $I_p = 0.09$ - $0.33\ MA$). In order to distinguish small-scale oscillations in the T-10 tokamak from previously analysed instabilities induced by intensive electron beams in nonthermal plasma (formed in discharges with low density, powerful auxiliary heating, and, in particular, during non-inductive current drive) present experiments generally considers Ohmically heated plasma with relatively high electron density [central line-averaged density $<n_e>$ up to ~ $(4.5\text{-}5.0)\ 10^{19}\ m^{-3}$].

2. Experimental results

Small-scale perturbations are analysed with the use of a toroidally viewing x-ray array [6], standard x-ray tomographic systems [4], x-ray gas detectors, and fast magnetic probes [1] (see Fig. 1). Additional *NaI(Tl)* monitor (placed outside the tokamak vessel) is used for measurements of the nonthermal ($E_\gamma \sim 0.5\text{-}3\ MeV$) x-ray and neutrons radiation. Spectrum of the x-ray radiation is identified using germanium pulse-height-analysis (*PHA*) system.

Tangential x-ray array (*TX - array*) is placed inside the tokamak vacuum vessel at the low field side of the torus bellow the equatorial midplane [see (1) in Fig. 1]. The system consists of the Si and CdTe x-ray detectors with Soller collimators placed inside protection container at the top of the movable rod. The detectors provide measurements of the emissivity fluxes in energy range ($E_\gamma \sim 2.5\text{-}\ 200\ keV$) with spatial and time resolution of order of $\delta r \sim 7\ mm$ and $3\ \mu s$, accordingly. Additional x-ray detector (*txhxr*) is placed in TX array inside sealed stainless-steel container (thickness of the wall is $\delta \sim 4$ - $5\ mm$) for monitoring the nonthermal x-ray emission ($E_\gamma > 45\ keV$).

Small-scale plasma perturbations are generally observed prior to the density limit disruptions in ohmically heated plasma. The evolution of the plasma parameters in the experiment is shown in Fig. 2. Similarly to a "classical" disruptions at high density (see [5]), additional gas puff at the quasi-stationary stage of discharge (see, $t > 700\ ms$ in Fig. 2) is accompanied by increase of the total radiated power and intensive cooling of the plasma edge. Subsequent erosion of the electron temperature profile outside the $q=2$ surface leads to formation of an unstable plasma configuration with explosive growth of the MHD perturbations and rapid loss of the stored plasma energy during an energy quench (see $t \sim 751.2\ ms$ in Fig. 2). The final stage of the disruption is accompanied by enhanced radiation due to plasma-wall interaction and strong impurities influx. The process is completed with decay of the plasma current, I_p, strong increase of the loop voltage, U_l, and bursts of the hard x-ray emission, I_{HXR}. Tomographic analysis of the x-ray emissivity measured using conventional x-ray arrays (*XRA, XRB, XRC*) indicated that energy quench is proceeded by joint rotation of the coupled $m=1,\ n=1$ and $m=2,\ n=1$ perturbations (see detailed analysis of the process in [4]). Growth of the coupled MHD perturbations is also accompanied by slowing down of the mode rotation. This is shown in Fig. 2(d) representing time evolution of the x-ray intensity measured using conventional (*xra07, xra16, xrb18*) and tangentially viewing x-ray arrays (*txray1, txray4*), accordingly. The large-scale m=2,n=1 perturbations are rotating in the case in the electron diamagnetic drift direction.

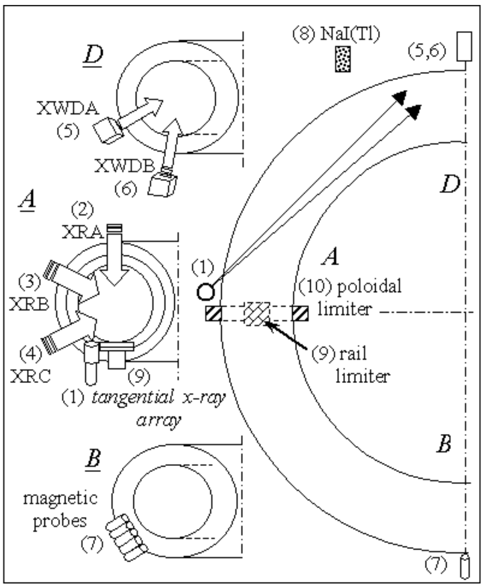

FIG. 1. Schematic view of the diagnostics in the T-10 tokamak. Small-scale oscillations and MHD modes are analysed by means of the tangential x-ray array, TX (1), standard x-ray tomographic arrays XRA (2), XRB (3), XRC (4), x-ray gas detectors XWDA, XWDB (5,6), and fast magnetic probes (7). Hard x-ray emission is measured by the *NaI(Tl)* monitor (8). Plasma in T-10 is restrained by a movable rail limiter (9) and guard poloidal limiter (10).

The MHD modes are additionally superimposed with small-scale x-ray perturbations observed most clearly prior to the energy quench using tangentially viewing x-ray array [see, oscillations with repetition rate $f_{SSO} \sim 19 - 20\ kHz$ in trace *txray4* in Fig. 2(e)]. The small-scale oscillations can be also identified with the conventional x-ray array [see, mark (1) in Fig. 2(e)], while amplitude of the x-ray perturbations is extremely small in the case (see bellow).

The small-scale x-ray perturbations shown in Fig. 2(e) represent example of quasi-continuous x-ray oscillations. Spectrogram of the tangential x-ray intensity is shown in the case in Fig. 3(b). The oscillations are represented by a solitary harmonic in spectrum of perturbations accompanying the *m=2, n=1* mode [see Fig. 3(b)]. Absence of side-band harmonics is in sharp contrast with broad-band spectrum of x-ray perturbations induced during energy quench later in the discharge [see, *t > 751.2 ms* in Fig. 3(b)].

Analysis of the plasma disruptions in discharges with various density, plasma current , and magnetic field [$<n_e> \sim (2.5 - 6)\ 10^{19} m^{-3}$, $I_p \sim 0.09 - 0.35$ MA, $B_t \sim 2.0 - 2.5$ T], made so far, indicated no clear dependence of small-scale oscillations on the plasma parameters, while repetition rate of the oscillations can be changed considerably in various plasma conditions ($f_{SSO} \sim 15 - 85$ kHz). Experiments indicate that repetition rate of the oscillations can be increased in plasma with high frequency of the *m=2* mode rotation [see, open circles in Fig. 3(c)]. Repetition rate f_{SSO} is typically twenty times higher than frequency of the m=2,n=1 mode.

Limited number of the tangentially viewing x-ray detectors in present experiments did not allow one to reconstruct internal structure of the small-scale x-ray perturbations. However, measurements of x-ray oscillations in series of consecutive tokamak discharges with similar plasma parameters using TX detectors with various lines of sights indicated that amplitude of the small-scale oscillations are generally increased around the

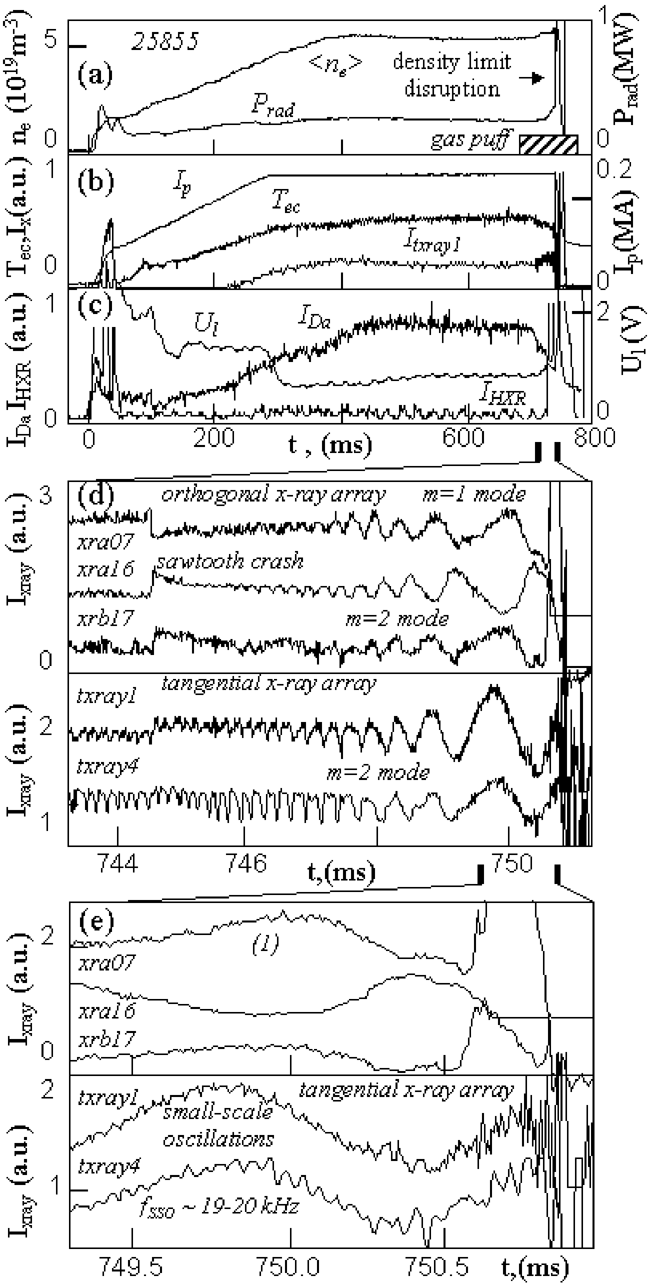

FIG. 2. *(a-c)* Time evolution of the plasma parameters during a density limit disruption in an ohmically heated plasma. Here, $<n_e>$ is the line averaged electron density, P_{rad} the total radiated power, I_p the plasma current, T_{ec} the electron (ECE) temperature, I_{txray1} the x-ray intensity measured by the tangential x-ray detector, U_l the loop voltage, I_{Da} the visible light (D_α) radiation from the limiter, and I_{HXR} the hard x-ray intensity. *(d-e)* Time evolution of the x-ray intensity measured by a conventional x-ray detector (*xra07, xra16, xrb17*) and by the tangential TX array (*txray1, txray4*) just prior to the energy quench. Small-scale oscillations (f_{SSO} ~ *19-20 kHz*) are observed simultaneously with slowly rotating m=2,n=1 and m=1,n=1 MHD modes.

$m=2,n=1$ mode [7].

Small-scale oscillations identified with the TX-array are also observed with the use of fast magnetic probes. This is illustrated in Fig. 4 representing time evolution of the poloidal magnetic field perturbations at five poloidal locations (see, probes *m1 - m5*) prior to the energy quench at the same density limit disruption as one shown in Fig. 3. Similarly to the x-ray measurements, small-scale magnetic oscillations are clearly observed just prior to the energy quench (see, *t ~ 749 - 751 ms* in Fig. 4) while they are not well identified at the earlier stage of the discharge (see, *t ~ 745.0 - 745.2 ms* in Fig. 4). The small-scale magnetic perturbations are typically characterised by the same phase shift as one of the m=2,n=1 mode (see dashed lines at time *t3, t4, t7, t8* and *t1, t2*, accordingly). This can probably indicate rotation of the small-scale oscillation in the same direction as one of the m=2 mode. However, phase shifts of the small-scale perturbations can be changed dramatically in subsequent cycles of the oscillations (see, dashed lines with no poloidal phase shift at time *t6* and *t10* in Fig. 4). Small phase-shifts ($\delta\phi \sim 0$) indicate that magnetic perturbation at the moments are symmetric in poloidal direction, while their repetition rate is up to 20 times higher than one of the m=2,n=1 mode. This fact seems contradicts assumption about possible connection of the small-scale perturbations with micro-tearing modes [1].

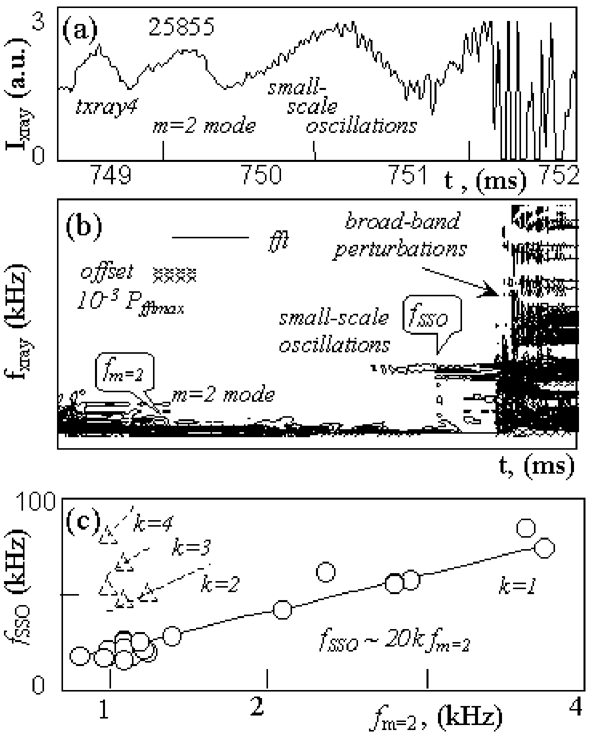

FIG. 3. Time evolution (a) and spectrogram (b) of the x-ray intensity measured by the tangential x-ray array. Quasi-coherent small-scale oscillations are represented by a solitary harmonic (f_{SSO} ~ *19-20 kHz*) in the perturbation spectrum accompanying the m=2 mode. (c) Repetition rate of the oscillations f_{SSO} in the plasma with various rotation frequency of the m=2,n=1 mode, $f_{m=2}$. In some cases, oscillations with extremely small amplitude are observed at higher frequencies [see dashed rectangles, in frame (c)]. These high frequency oscillations are not well resolved by the present diagnostic techniques and are not studied here in details. Solid and dashed lines in frame (c) represents relation $f_{SSO} \sim 20\, k f_{m=2}$, for *k=1,2, 3, 4*, accordingly.

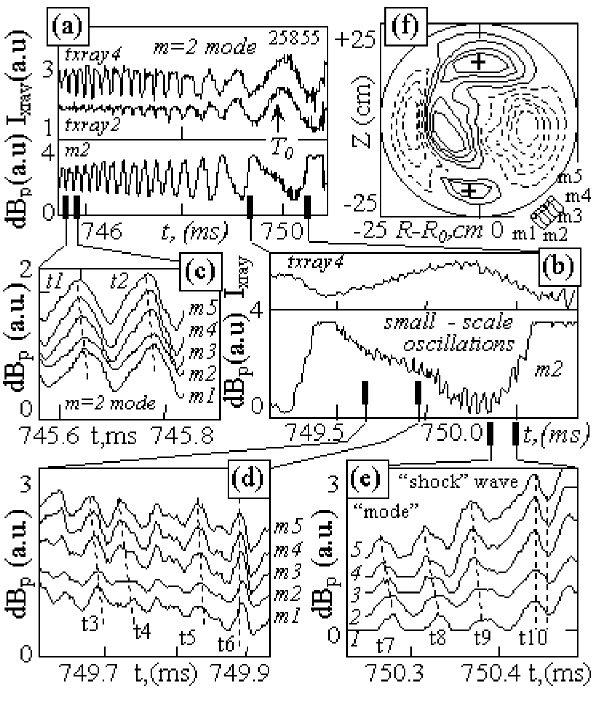

FIG. 4. (a-e) Time evolution of the poloidal magnetic field perturbations, dB_p, measured prior to the density limit disruption using five magnetic probes (*m1, m2, m3, m4, m5*) with tight poloidal separation. Also shown is the x-ray intensity, *txray4*, measured using the TX array. Frame (b) represents the tomographically reconstructed image of the x-ray perturbations measured using conventional x-ray arrays (XRA,XRB, XRC) at time T_0 = *750.096 ms*.

Small-scale x-ray oscillations are typically localised around the *m=2,n=1* mode in the outer part of the plasma. No direct connection of the oscillations with the internal *m=1,n=1* perturbations is observed so far in experiments in the T-10. In plasma with high density amplitude of the small-scale x-ray oscillations can be enhanced temporarily just after a sawtooth crash. The oscillations are observed in the case as wavelet-like x-ray bursts localised in plasma area outside the sawtooth inversion radius (see Fig. 5). The wavelet x-ray bursts is initiated when plasma perturbations (induced during a sawtooth crash around the sawtooth inversion radius) reach plasma area close to localisation of the *m=2* mode. Appearance of wavelet-like x-ray oscillations during a sawtooth crash indicates that perturbations can be probably connected with destabilisation of the secondary magnetic islands due to interaction of large-scale MHD modes with various helicities (e.g., coupling of the *m=1,n=1* and *m=2,n=1* modes). However, calculations indicated that several side-band harmonics should be destabilised simultaneously in the case. This seems contradict the solitary nature of the small-scale oscillations observed in the experiments.

Experiments in the T-10 indicted no considerable difference in behaviour of the small-scale oscillations prior to density limit disruptions in ohmically and ECRH heated plasma [7]. Small-scale x-ray oscillations during auxiliary heating are generally characterised by faster repetition rate possibly connected with higher rotation frequency of the m=2 mode.

While small-scale x-ray perturbations can be observed as continuous quasi-coherent oscillations their amplitude is typically increased at the growing phase and at the top of the m=2,n=1 mode. Maximum amplitude of the small-scale oscillations in the case is comparable with one of the m=2 perturbations. Appearance of the small-scale oscillations at maximum of the perturbation due to the MHD mode is phenomenologically similar to ballooning modes observed previously in disruptions at high β [2]. However, ballooning origin of the perturbations can be possibly excluded in present analysis due to relatively low magnetohydrodynamic pressure ($\beta_p \sim 0.05$) in the T-10 plasma and continuous growth of the oscillations in respect to various phases of the *m=2* mode observed in some cases (see Fig. 3).

Small scale oscillations prior to the disruption are sometimes observed using hard x-ray detector placed inside the tokamak vessel (see Fig. 6). Perturbations observed with the hard x-ray detector are

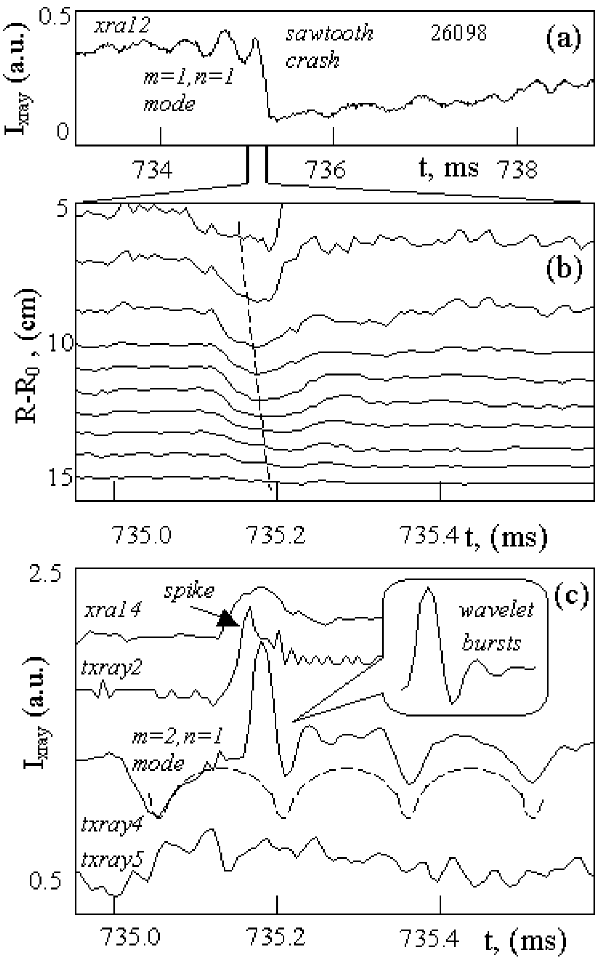

FIG. 5. Time evolution (a) and contour plot (b) of the x-ray intensity measured with the orthogonal x-ray array XRA. The x-ray perturbations induced during the sawtooth crash (*t = 735.15 ms*) are observed with time delay at outer radii (see dashed line in frame (b). (c) Time evolution of the x-ray intensity measured with the tangential x-ray array (*txray2, txray4, txray5*). Wavelet-like burst of small-scale oscillations is induced during the crash in plasma area around the m=2,n=1 MHD mode (see *txray4*). Dashed line in frame (c) represents schematically perturbations of the x-ray intensity due to a singular m=2 mode.

typically characterised by delay in respect to oscillations measured with collimated TX detectors [see, accordingly *txhxr* and *txray2* in Fig. 6 (b)]. Such delay, as well as different phases of the oscillations measured with various TX detectors, indicate that small-scale perturbations can not be represented by a simple pickup of hard x-ray radiation generally observed in tokamaks due to plasma-wall interaction during a disruption.

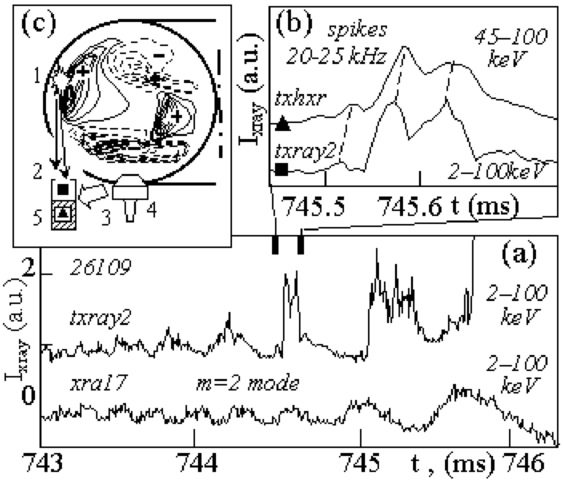

FIG. 6. (a, b) Time evolution of the x-ray intensity (E_γ ~ *2 - 100 keV*) measured by the tangential (*txray2*) and orthogonal (*xra17*) arrays and suprathermal x-ray radiation (E_γ ~ *45 – 100 keV*) measured by the in-vessel "hard" x-ray detector (*txhxr*). (c) Tangentially integrated x-ray perturbations calculated for the modelled singular m=2,n=1 mode. Internal x-ray bursts (1) are initially identified by the TX array (2), while hard x-ray radiation (3) induced by the possible interaction of the electron beams with the limiter (4) is measured with time delay using shielded detector (5).

Repetitive growth of the small-scale oscillations prior to the disruption is phenomenologically similar to intensive bursts of the nonthermal x-ray radiation often accompanied density limit disruptions in the T-10 tokamak [6]). Studies of the phenomena in previous experiments revealed possible connection of the bursts with beams of the nonthermal electrons (E_γ ~ *20 – 100 keV*) generated around X-points of the *m=2,n=1* magnetic islands [6]. In contrast to small-scale x-ray oscillations, the bursts are typically characterised by extremely high intensity of the x-ray radiation (amplitude of the x-ray perturbation is up to 50-100 times higher than one of the thermal oscillations due to the m=2 mode). Intensive x-ray bursts are typically observed at the growing phase and at maximum of the *m=2* perturbations, which is remarkably similar to small-scale oscillations. Moreover, amplitude of x-ray intensity during a single burst is often modulated with repetition rate close to one of the small-scale oscillations, observed earlier in the discharge. This indicates, indirectly, that small-scale oscillations can be in part connected with beams of the nonthermal electrons.

Possible connection of the small-scale x-ray perturbations with classical acceleration of the electron beams in longitudinal equilibrium electric field can be checked in experiments with additional current ramp up just prior to the disruption at high density (see Fig. 7). Growth of the plasma current is accompanied in the case by considerable increase of the longitudinal electric field at the outer part of the plasma. (Loop voltage is increased from quasi-stationary value $U_l \sim 1.5\ V$ up to $U_l \sim 16\ V$ just prior to the energy quench and further up to $U_l \sim 70\ V$ during disruption. It should be pointed out that power supply system used in T-10 for control of plasma current is capable to provide increase of the loop voltage even after the energy quench.) The process should be accompanied by amplification of runaways electron beams with possible subsequent increase of the x-ray bursts amplitude. However, no considerable difference in amplitude of the x-ray perturbation prior to the energy quench is observed in the experiments. While present experiments can not provide detailed information for qualitative analysis of the runaway electrons in experiments with current ramp-up, it seems that increased loop voltage during current ramp-up (in the analysed U_l - range) does not change considerably initial stage of the disruption.

3. Conclusions

In this paper, we have discussed a new type of small-scale oscillations accompanying the growth of MHD modes prior to density limit disruptions in the T-10 tokamak. The small-scale oscillations are represented by a solitary harmonic in a spectrum of perturbations accompanying the m=2,n=1 mode and are typically localised around X-points of the magnetic islands. During the energy quench the quasi-coherent perturbations are transformed to intensive bursts of the suprathermal x-ray radiation. The correlation of the small-scale oscillations with localised beams of nonthermal electrons analysed in the present experiments can possibly represent a general phenomena, accompanying disruptions in tokamaks, not analysed previously in detail due to diagnostic limitations.

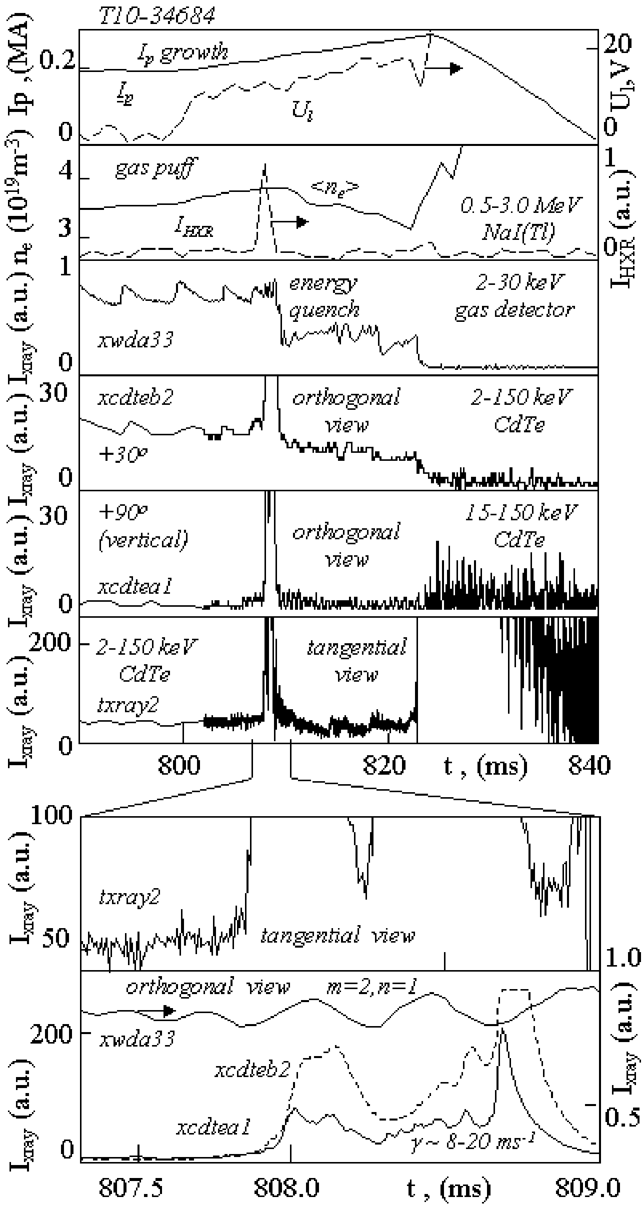

FIG. 7. Time evolution of plasma parameters in experiments with ramp-up of plasma current, I_p, just prior to the density limit disruption. Here, U_l is loop voltage, $\langle n_e \rangle$ line averaged electron density, I_{HXR} hard x-ray intensity, I_{xray}*(xwda33)* x-ray intensity measured using XWDA gas detector. Also shown, intensity of the x-ray radiation measured using CdTe detectors with orthogonal (*xcdtea1*, *xcdteb2*) and tangential (*txray2*) view of the plasma column.

Acknowledgements

The author would like to thank A. Ya. Kislov, Y. D. Pavlov, V. S. Strelkov for support of the experiments and Yu. N. Dnestrovskij, S. V. Mirnov, V. I. Poznyak, K. A. Razumova, I. B. Semenov, for critical discussion of the experimental results. The work is supported by Russian Atomic Energy Agency ROSATOM.

References:

[1] VOLKOV, V.V. et al., Soviet Journal of Plasma Physics 16, (1990) 295.
[2] FREDRICKSON, E. D., et al., Physics of Plasmas 3, (1996) 2620.
[3] BISKAMP, D., Nonlinear magnetohydrodynamic, Cambridge University Press, Cambridge (1993).
[4] SAVRUKHIN, P. V., et al., Nucl. Fusion, 34, (1994) 317.
[5] ITER Physics Expert Group on Disruptions, Plasma Control, and MHD, ITER Physics Basis Editors, Nucl. Fusion 39, (1999) 2251.
[6] SAVRUKHIN, P. V., Phys. Rev. Lett. 86, 3036 (2001).
[7] SAVRUKHIN, P. V., et al., Phys. Rev. Lett. 92, (2004) 095002.
[8] GILL, R. D., et al., Nucl. Fusion 40, (2000) 163.